

Diversification of Acrylamide Polymers via Direct Transamidation of Unactivated Tertiary Amides

Lucca Trachsel, Debabrata Konar, Jason D. Hillman, Cullen L. G. Davidson, IV, and Brent S. Sumerlin*



Cite This: *J. Am. Chem. Soc.* 2024, 146, 1627–1634



Read Online

ACCESS |



Metrics & More

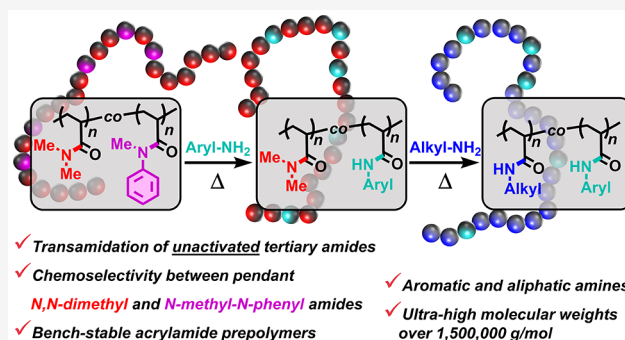


Article Recommendations



Supporting Information

ABSTRACT: Postpolymerization modification offers a versatile strategy for synthesizing complex macromolecules, yet modifying acrylamide polymers like poly(*N,N*-dimethylacrylamide) (PDMA) is notoriously challenging due to the inherent stability and low reactivity of amide bonds. In this study, we unveil a novel approach for the direct transamidation of PDMA, leveraging recent advances in the transamidation of unactivated tertiary amide substrates. By exploiting photoiniferter polymerization, we extended this direct transamidation approach to ultrahigh-molecular-weight (UHMW) PDMA, showcasing the unprecedented postpolymerization modification of synthetic polymers exceeding 10^6 g/mol. We also designed acrylamide copolymers comprising both the moderately reactive *N*-methyl-*N*-phenyl tertiary amides, along with the less reactive, fully alkyl-substituted *N,N*-dimethyl amides inherent to PDMA. This disparate reactivity enabled a sequential, chemoselective transamidation by initially targeting the more reactive pendant aryl amides with less nucleophilic aromatic amines, and second, transamidating the untouched *N,N*-dimethyl amide moieties with more nucleophilic aliphatic amines, yielding a uniquely diversified acrylamide copolymer. This work not only broadens the scope of postpolymerization modification strategies by pioneering direct transamidation of unactivated amides but also provides a robust platform for the design of intricate macromolecules, particularly in the realm of UHMW polymers.



INTRODUCTION

In recent decades, the evolution of postpolymerization modification (PPM) strategies has been markedly shaped by breakthroughs and advancements in highly efficient chemoselective transformations.^{1–6} PPM facilitates the synthesis of complex macromolecules by transforming pendent reactive groups of polymers into desired functionalities after polymerization, allowing for the synthesis of (co)polymers that are otherwise unobtainable by direct polymerization and the precision tuning of polymer properties that are different from their parent polymers.^{7,8} PPM strategies involving nucleophilic substitution, specifically for polymers with electrophilic carbonyls like activated esters found in poly(*N*-hydroxysuccinimide-(meth)acrylate) and poly(pentafluorophenyl(meth)acrylate), are among the most well-established techniques.^{9,10} Despite the ability to modify these reactive precursor polymers under relatively mild conditions, their drawbacks—including poor atom economy, the need for functional monomer synthesis, and vulnerability to hydrolysis—have driven the exploration of alternative techniques.¹¹ One such technique is the organocatalyzed transesterification and amidation of nonactivated ester-containing polymers such as poly(methyl acrylate).^{12,13}

In contrast, PPM of poly(meth)acrylamides has received considerably less attention due to the high stability and

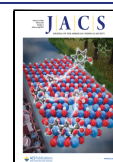
reduced reactivity of amides toward nucleophiles. The diminished electrophilicity of amide moieties is primarily attributed to their high resonance energy (15–20 kcal/mol), stemming from the delocalization of the nitrogen lone pair electrons into the π^* orbital of the carbonyl group ($\pi^*_{C=O}$) resulting in significant planarity and stabilization of amides.^{14,15} Ground-state destabilization as a means to increase the electrophilicity of amides has been achieved via geometric alteration through twisting as well as electronic activation.^{16,17} Inspired by recent developments in amide bond activation and direct N–C(O) bond cleavage by the Szostak group,^{18,19} Hillmyer and co-workers reported the PPM of acrylamide polymers, specifically poly(*N,N*-bis(*tert*-butoxycarbonyl)-acrylamide) (poly(*N,N*-*boc*₂-acrylamide)), bearing twisted and electronically activated tertiary amides that allowed for the direct transamidation with different nucleophilic amines (Figure 1A).²⁰ Like previous PPM reports based on activated

Received: October 31, 2023

Revised: December 12, 2023

Accepted: December 13, 2023

Published: January 8, 2024



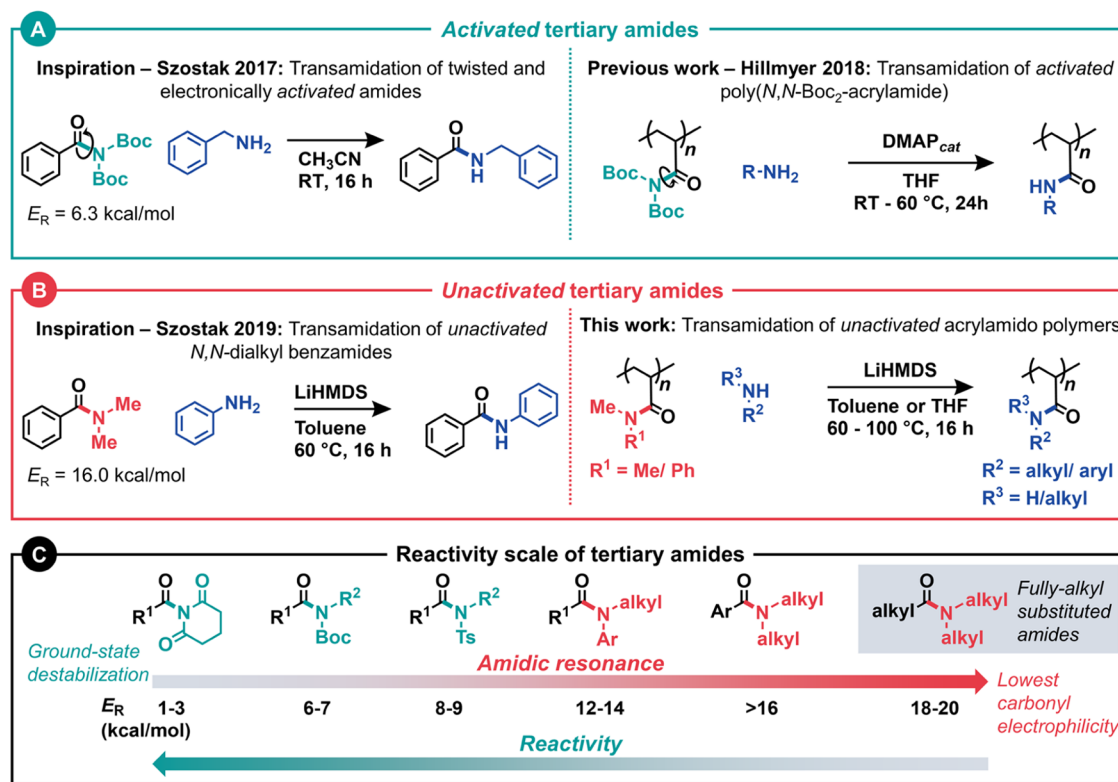


Figure 1. (A) Transamidation of activated tertiary amides such as *N,N*-Boc₂-benzamide has been achieved through ground-state destabilization, as initially reported by Szostak et al.^{18,19} This approach was subsequently applied to a macromolecular system by Hillmyer et al.²⁰ (B) Lithium hexamethyldisilazane (LiHMDS)-mediated transamidation of unactivated tertiary amides (with a resonance energy (E_R) of 15–20 kcal/mol) initially pioneered by Szostak et al.²¹ In this work, we subject conventional acrylamide polymers to transamidation by way of a novel PPM approach. (C) Reactivity spectrum of tertiary amides, ranging from the highly reactive ground-state destabilized twisted amides like *N*-acylglutarimides²² to the least reactive fully alkyl-substituted amides.²³

ester prepolymers, this approach relied on the tedious synthesis of a reactive electron-deficient monomer, which may limit polymerization scope and the shelf life of the resulting polymers.

We were inspired by the recent methodology reported by Szostak and co-workers,²¹ in which unactivated tertiary amides were shown to undergo lithium hexamethyldisilazane (LiHMDS)-mediated direct transamidation with a plethora of nucleophilic and non-nucleophilic amines. We sought to adapt this chemistry to the macromolecular realm, introducing for the first time diversification of unactivated acrylamide polymers (Figure 1B). We reasoned that the *N,N*-dimethyl amide moieties present in poly(*N,N*-dimethylacrylamide) (PDMA) could be subjected to the reaction conditions reported by Szostak et al. for small-molecule unactivated tertiary amide substrates to access functionalized acrylamide polymers.²¹ This would allow the use of otherwise very stable and chemically inert PDMA as a precursor polymer for PPM.

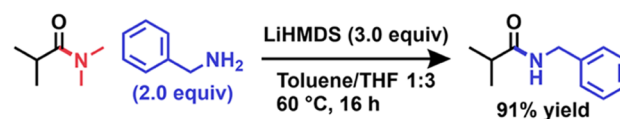
RESULTS AND DISCUSSION

We first sought to investigate the feasibility of the LiHMDS-mediated transamidation reaction conditions as reported by Szostak et al. for a fully alkyl-substituted tertiary amide substrate, a moiety acting as a suitable small-molecule mimic for the PDMA repeat units. Fully alkyl-substituted tertiary amides are considered the most thermodynamically stable amides, owing to their inherent planar geometry, highest C(acyl)–N rotation energy, and lowest carbonyl electrophilicity.^{19,24} Using *N,N*-dimethylisobutyramide bearing α -

branching at the carbon center as a small-molecule model surrogate for PDMA and benzylamine as the nucleophile, we successfully obtained the transamidated product in high yield in the presence of LiHMDS, a sterically hindered non-nucleophilic base that has recently been utilized in electrophilic amide bond activation.^{25–27} The reactions were carried out in toluene/THF at slightly elevated temperatures (Figures 2A, S1 and S2).

Encouraged by these initial results, we shifted our focus to the macromolecular system. Using photoiniferter polymerization,²⁸ a reversible-deactivation radical polymerization

A Proof-of-concept – Small molecule PDMA model



B Direct transamidation of PDMA

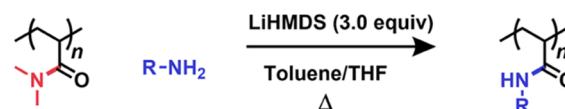


Figure 2. (A) Proof-of-concept experiment demonstrating the feasibility of direct transamidation mediated by LiHMDS on a fully alkyl-substituted tertiary amide, specifically using *N,N*-dimethylisobutyramide as a model for PDMA repeat units. (B) LiHMDS-mediated transamidation of PDMA using various amine nucleophiles.

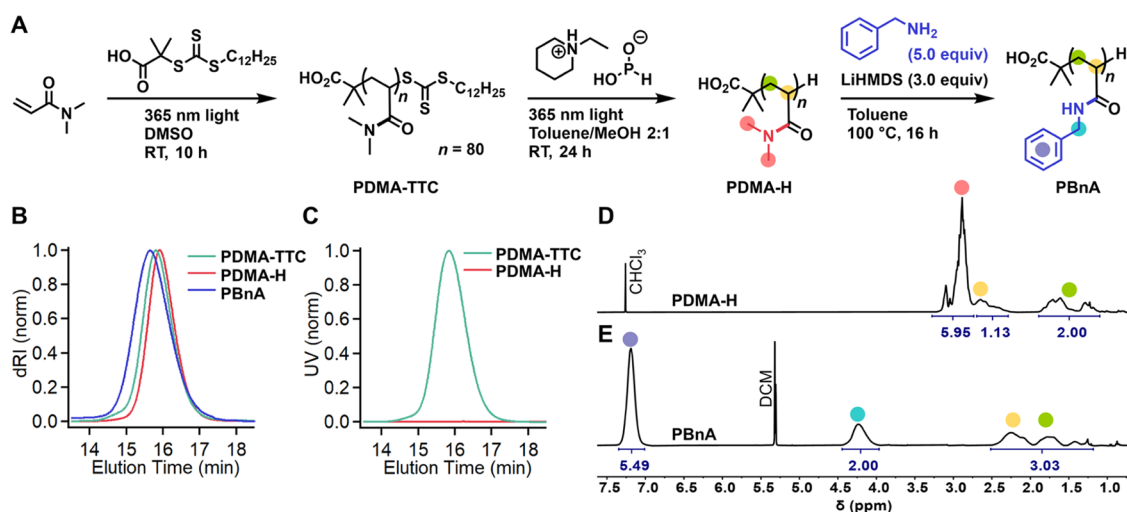


Figure 3. (A) Reaction scheme of photoiniferter polymerization of DMA and subsequent photolytic TTC end-group removal to obtain PDMA-TTC and PDMA-H, respectively. Lastly, LiHMDS-mediated direct transamidation of PDMA-H with benzylamine to yield PBnA. (B) Overlaid differential refractive index (dRI) SEC traces of PDMA-TTC, PDMA-H, and the transamidated polymer PBnA. (C) Overlaid UV SEC traces of PDMA-TTC and PDMA-H, confirming the removal of the TTC end-group. (D) ^1H NMR spectrum of PDMA-H and (E) ^1H NMR spectrum of PBnA after transamidation of PDMA-H with benzylamine, showing the complete disappearance of the peaks of the N,N -dimethyl amide moieties of PDMA at $\delta = 2.8$ ppm.

(RDRP) technique,^{29–31} we synthesized well-defined low-molecular-weight PDMA with a number-average molecular weight ($M_{n,\text{SEC}}$) of $8.2 \text{ kg}\cdot\text{mol}^{-1}$ and a dispersity (D) of 1.03 as determined by size-exclusion chromatography (SEC) (Figure 3A). This substrate allowed us to probe the direct transamidation of polymers featuring fully alkyl-substituted N,N -dialkylamides (Figure 2B). To preclude aminolysis and potential side reactions involving the trithiocarbonate (TTC) end group in subsequent transamidation processes, we photolytically removed the TTC by exposing PDMA-TTC to long-wave UV light in the presence of a hydrogen atom donor, resulting in PDMA with hydrogen end groups (PDMA-H).³² SEC analysis confirmed the successful end-group removal, evidenced by the disappearance of the UV signal at 320 nm in the trace of PDMA-H (Figure 3C). Additionally, no noticeable alteration in molecular weight and distribution was observed, as shown by the overlaid refractive index (RI) traces of PDMA-TTC and PDMA-H (Figure 3B).

We then sought to apply the direct transamidation approach to PDMA-H, employing the reaction conditions initially used for the small-molecule analog. Specifically, we used benzylamine (2.0 equiv relative to the N,N -dimethyl amide moieties of PDMA) and LiHMDS (3.0 equiv) in a toluene/THF mixture at 60°C . Encouragingly, we achieved a 42% conversion in the polymer system, as confirmed by ^1H NMR spectroscopy (Figure S9). Further optimization was performed (Table S1, Figures S10–S19), which led to a quantitative transamidation to poly(N -benzylacrylamide) (PBnA) when the nucleophile excess was increased to 5.0 equiv and the reaction temperature was elevated to 100°C in toluene (Figure 3A). ^1H NMR spectroscopy revealed the complete disappearance of the N,N -dimethyl protons and the emergence of the characteristic protons of N -benzyl amide (Figure 3D,E). Furthermore, the SEC trace for PBnA displayed a shift to lower elution times, indicating an increase in molecular weight ($M_{n,\text{SEC}} = 13.5 \text{ kg}\cdot\text{mol}^{-1}$ and $D = 1.03$) relative to the parent PDMA-H (Figure 3B).

As compared to other approaches for efficient synthetic upcycling of low-reactivity polymers that often rely on continuous removal of byproducts to drive the equilibrium,^{12,33,34} our strategy resembles others³⁵ that occur through an irreversible mechanism, obviating the need for specialized experimental setups. Indeed, density functional theory calculations on small-molecule substrates revealed that the N-H bond in the secondary amide product undergoes deprotonation by LiHMDS, resulting in a stable amidate lithium complex, a process that helps to thermodynamically drive the overall transformation.²¹ The necessity of using an excess of LiHMDS (3.0 equiv) for complete transamidation with benzylamine is underscored by the diminished conversion (59%) when only 1.0 equiv of LiHMDS and otherwise identical reaction conditions were employed (Table S1, entry S8, and Figure S16).

Notably, the absence of LiHMDS resulted in only 30% conversion and poor selectivity, as evidenced by the appearance of additional peaks in the NMR spectrum (Figure S15). In contrast, no transamidation occurred at room temperature even with LiHMDS, underscoring the critical role of both elevated temperature and LiHMDS for the direct transamidation of PDMA with benzylamine (Figure S14). This observation aligns with expectations of a heightened kinetic barrier in the macromolecular system due to increased steric hindrance compared with small-molecule reactions.

With optimal conditions in hand, we proceeded to expand the substrate scope of the direct transamidation of PDMA. Utilizing high-boiling-point primary amines like 3-phenyl-1-propylamine and n -hexylamine, we achieved quantitative conversion ($>95\%$), as confirmed by ^1H and 2D ^1H - ^{13}C heteronuclear single-quantum correlation (HSQC) NMR spectroscopy (Figure 4, Figures S20–S24). More sterically hindered primary amines, such as cyclohexylamine, gave 70% conversion (Figure S25). Moreover, functional groups like methoxy and tertiary amines, present in 2-methoxyethylamine and N,N -dimethylethylenediamine, respectively, were tolerated, resulting in more than 80% conversion to the

Entry	R ¹	Nucleophile ^a	Conversion ^b (%)
1	Me		>95
2	Me		>95
3	Me		>95
4	Me		69
5	Me		83
6	Me		90
7	Me		50
8	Me		trace
9	Me		trace
10	Me		48
11	Me		47
12	Ph		71
13	Ph		>95
14	Ph		80

Figure 4. Amine scope of the LiHMDS-mediated direct transamidation of poly(*N,N*-dimethylacrylamide) for R¹ = Me and poly(*N*-methyl-*N*-phenylacrylamide) for R¹ = Ph. Reaction conditions for R¹ = Me: toluene at 100 °C and 5.0 equiv of ^aamine nucleophile; for R¹ = Ph: toluene/THF (2:3) at 60 °C and 2.0 equiv of ^aamine nucleophile. ^bConversion was determined using ¹H NMR spectroscopy.

corresponding transamidated acrylamide polymers (Figures 4, S26 and S27). Conversely, using furfuryl amine, despite its similar p*K*_a and nucleophilicity to benzylamine, we achieved only moderate conversion of 50% (Figure S28). While less efficient, secondary amines such as *N,N*-dibutylamine and 4-methylpiperidine were also capable of transamidation of PDMA, achieving moderate conversion (Figures S29 and S30). Less nucleophilic aromatic amines like aniline and 4-methoxyaniline yielded only trace amounts of transamidation, a finding confirmed on our small-molecule PDMA model substrate.

Attempting to transamidate the fully alkyl-substituted tertiary amide, *N,N*-dimethylisobutyramide, using 4-methoxyaniline resulted in low conversions, even after extended reaction times for 2 days at elevated temperatures (Figures S31 and S32). LiHMDS-mediated transamidation of tertiary alkyl amides with less nucleophilic aromatic amines proved to be thermodynamically unfavorable.³⁶ This is exacerbated by the electron-donating nature of the three alkyl groups (R₁₋₃) present in fully aliphatic tertiary amides (R₁-C(=O)-N(R₂)-R₃), which further diminish the reactivity of these amides toward nucleophilic acyl substitution.³⁷ This result sharply contrasts with the high efficiency of LiHMDS-mediated transamidation observed in small-molecule tertiary amides with aryl substituents, such as *N,N*-dimethylbenzamide, with anilines, as demonstrated by the Szostak group (Figure 1B).²¹

To date, the PPM of synthetic ultrahigh-molecular-weight (UHMW) polymers, specifically those with molecular weights exceeding 10⁶ g·mol⁻¹, has not been reported, despite growing

interest in engineering functional UHMW polymers to better mimic the size of naturally occurring macromolecules such as mucins and lubricins.³⁸⁻⁴⁰ We reasoned that recent advances in accessing UHMW acrylamide and (meth)acrylate polymers through photoiniferter polymerization,^{41,42} particularly PDMA,^{43,44} along with the direct transamidation of PDMA, paves the way for new opportunities in the diversification of UHMW polymers. As a proof of concept, we subjected well-defined UHMW PDMA (*M*_{n,SEC} = 1220 kg·mol⁻¹, *D* = 1.14, degree of polymerization (*DP*_n) = 12,000) synthesized by photoiniferter polymerization to the optimized transamidation conditions using benzylamine in the presence of LiHMDS (Figure 5A). Subsequent ¹H NMR spectroscopy revealed the

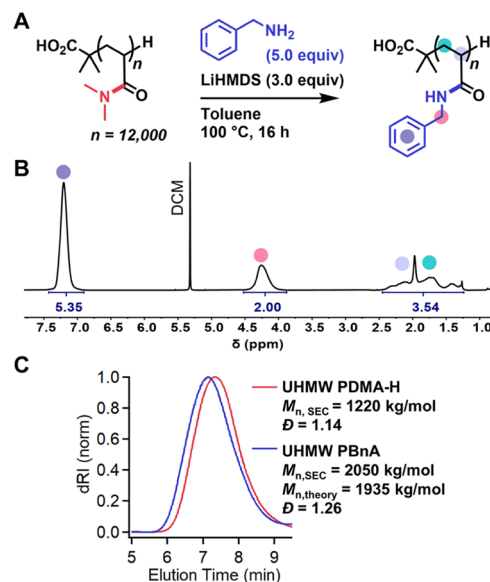


Figure 5. (A) Reaction scheme for the LiHMDS-mediated transamidation of UHMW PDMA with benzylamine to obtain UHMW poly(*N*-benzylacrylamide) (PBnA). (B) ¹H NMR spectrum of transamidated UHMW PBnA, recorded in DCM-*d*₂. (C) Overlaid SEC traces of the UHMW PDMA and UHMW PBnA showing the shift to lower elution time upon transamidation.

quantitative conversion of UHMW PDMA to the transamidated UHMW PBnA, evident from the appearance of the characteristic proton peaks corresponding to PBnA (Figures 5B and S33). Notably, SEC analysis of the transamidated UHMW polymer indicated an increase in molecular weight (*M*_{n,SEC} = 2050 kg·mol⁻¹, *D* = 1.26), aligning closely with the theoretical molecular weight (*M*_{n,theory} = 1935 kg·mol⁻¹) predicted by ¹H NMR spectroscopy, assuming complete transamidation (Figure 5C). Remarkably, the SEC trace of the UHMW PBnA remained monomodal with relatively low *D* after the transamidation process, suggesting the absence of side reactions that would lead to polymer degradation or cross-linking and reinforcing the feasibility of LiHMDS-mediated direct transamidation for acrylamide polymers in the UHMW range. Notably, attempts to directly polymerize *N*-benzylacrylamide targeting UHMW (*DP*_n = 12,000) under optimal photoiniferter conditions resulted in polymers with significantly lower molecular weights than expected, as evidenced by the marked discrepancy between the measured *M*_{n,SEC} = 204 kg·mol⁻¹ and theoretical *M*_{n,theory} = 1670 kg·mol⁻¹, along with broad molecular weight distributions (*D* > 2) (Figure S32). These findings demonstrated an uncontrolled polymerization,

potentially attributed to chain transfer to a monomer involving benzylic hydrogen abstraction. This emphasizes the merit of directly transamidating readily accessible UHMW PDMA as a promising approach to obtaining a broad range of UHMW acrylamide polymers.

In pursuit of expanding the reaction scope of this transamidation method to accommodate less nucleophilic aromatic amines, we sought to incorporate *N*-alkyl-*N*-aryl tertiary amides into acrylamide polymers. These aryl amides exhibit enhanced reactivity toward direct acyl *N*-C(O) bond cleavage with less nucleophilic aromatic amines, compared to fully alkyl-substituted tertiary amides like the *N,N*-dimethyl amides found in PDMA.⁴⁵ Specifically, we synthesized *N*-methyl-*N*-phenyl-acrylamide (MPA) which features an electron-withdrawing phenyl substituent on nitrogen, leading to resonance destabilization and thereby weakening the *N*-C(O) bond (Figures 6A, S3, and S4). For instance, the resonance

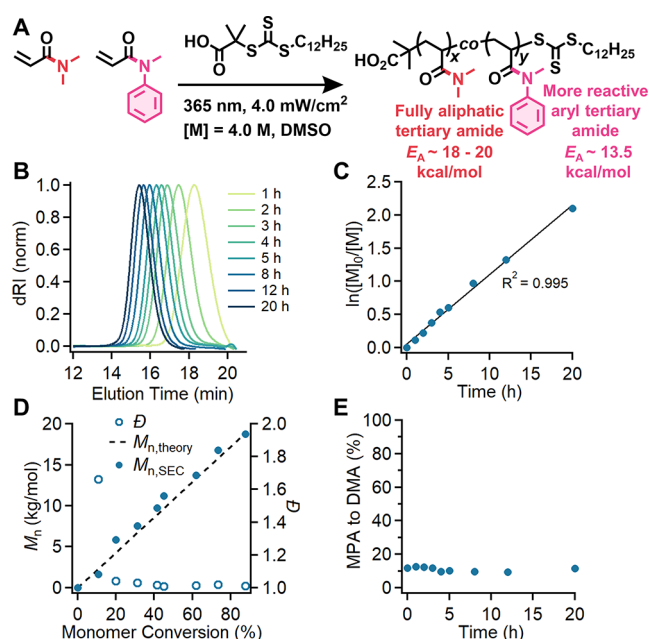


Figure 6. (A) Reaction scheme of the photoiniferter copolymerization of DMA and MPA. (B) Evolution of SEC traces over time during copolymerization showing monomodal shifts toward lower elution volumes. (C) Pseudo-first-order kinetics for the photoiniferter copolymerization of DMA and MPA using the averaged concentration of both monomers, where the black line indicates the linear fit with $R^2 = 0.995$. (D) $M_{n,SEC}$ versus monomer conversion showing good agreement with $M_{n,theory}$ up to high conversion while maintaining low dispersity (\bar{D}). (E) Ratio of unreacted MPA to DMA throughout the copolymerization, indicating proportional and statistical incorporation of each comonomer into the polymer.

stabilization of *N*-methyl-*N*-phenylbenzamide ($E_R = 13.5$ kcal/mol) is significantly lower than that of *N,N*-dialkyl tertiary amides, such as *N,N*-dimethylbenzamide ($E_R = 16.0$ kcal/mol) and *N,N*-dimethylacetamide ($E_R = 18.3$ kcal/mol).⁴⁶ Given that MPA has previously only been polymerized through metallocene-mediated coordination polymerization⁴⁷ and conventional radical polymerization methods in the context of stereoregular polymers,^{48,49} we initially explored the kinetics and control of copolymerizing MPA and DMA using photoiniferter polymerization. Our aim was to achieve varying molecular weights and levels of MPA incorporation, resulting in different P(DMA-*co*-MPA) copolymers (Figures 6A and

S33–S50). SEC analysis showed clean shifts of the traces to lower elution times as the polymer chains grew over the course of the copolymerization (Figure 6B). Additionally, the linear pseudo-first-order kinetics plot indicated a constant radical concentration throughout the copolymerization (Figure 6C). Moreover, $M_{n,SEC}$ showed a linear increase with conversion and aligned well with the theoretical number-average molecular weight determined by ¹H NMR spectroscopy ($M_{n,theory}$) (Figure 6D). All of these results together indicated that photoiniferter copolymerization of DMA and MPA was well controlled. Furthermore, ¹H NMR spectroscopy revealed that the molar ratio of unreacted MPA to DMA remained constant during copolymerization, suggesting that both monomers were incorporated at similar rates and were uniformly distributed along the polymer chain (Figure 6E). Statistical copolymerization of DMA and MPA was confirmed by determining the reactivity ratios of DMA ($r_{DMA} = 0.83$) and MPA ($r_{MPA} = 1.01$). This was achieved by applying a nonterminal fitting model to the monomer conversion versus time data, utilizing the Beekingham–Sanoja–Lynd (BSL) equations.⁵⁰ Detailed information regarding this analysis is provided in the ESI (Figure S63).

With the statistical copolymers in hand, we explored the LiHMDS-mediated transamidation using the less nucleophilic aromatic amine, 4-methoxyaniline, under modified reaction conditions, specifically THF/toluene mixture at 60 °C. Owing to the higher acidity of anilines ($pK_a = 25$ –30 in DMSO)^{51,52} compared to aliphatic primary amines ($pK_a = 35$ –40 in DMSO),⁵³ these derivatives undergo deprotonation when exposed to the strong base LiHMDS ($pK_a = 25.8$ in THF).⁵⁴ This required the use of a more polar and coordinating solvent, such as THF, to solubilize the likely formed lithium complex with the deprotonated aniline anion,²¹ suggesting that different mechanisms are at play in LiHMDS-mediated transamidation when using aliphatic versus aromatic amines. Remarkably, ¹H NMR spectroscopy revealed selective transamidation of the more reactive *N*-methyl-*N*-phenyl amide moieties of P(DMA-*co*-MPA) copolymers containing 5 or 50 mol % of MPA, while the DMA-derived amide remained unaffected, resulting in poly(DMA-*co*-*N*-(4-methoxyphenyl) acrylamide) (P(DMA-*co*-MeOPA)) (Figures S37–S40 and S48–S50). Additionally, the selectivity between DMA and MPA moieties was confirmed using 2D HSQC spectroscopy, which resolved overlapping signals in broad polymeric peaks evident in the ¹H NMR spectra (Figures S39, S49, and S50). This implies that the reactivity trend of tertiary amides, as dictated by the type of nitrogen substituent according to the work of Szostak et al., can also be applied to macromolecular systems.

Exploiting photoiniferter polymerization to access extraordinarily high DP_n , we also synthesized a UHMW version of P(DMA-*co*-MPA) featuring 10 mol % MPA ($M_{n,SEC} = 935$ kg mol⁻¹, $\bar{D} = 1.11$). SEC characterization revealed a uniform shift of molecular weight during the polymerization, polymers with low \bar{D} , and good agreement between experimental and theoretical molecular weights, all of which indicated controlled polymerization (Figure S53). Finally, we performed a sequential transamidation experiment of UHMW P(DMA-*co*-MPA), initially with 4-methoxyaniline and then with benzylamine, to demonstrate the chemoselectivity between pendent *N,N*-dimethyl and *N*-methyl-*N*-phenyl amide groups (Figure 7A). Following the first reaction with the less nucleophilic 4-methoxyaniline, ¹H NMR spectroscopy indicated complete transamidation of the *N*-methyl-*N*-phenyl amide moieties,

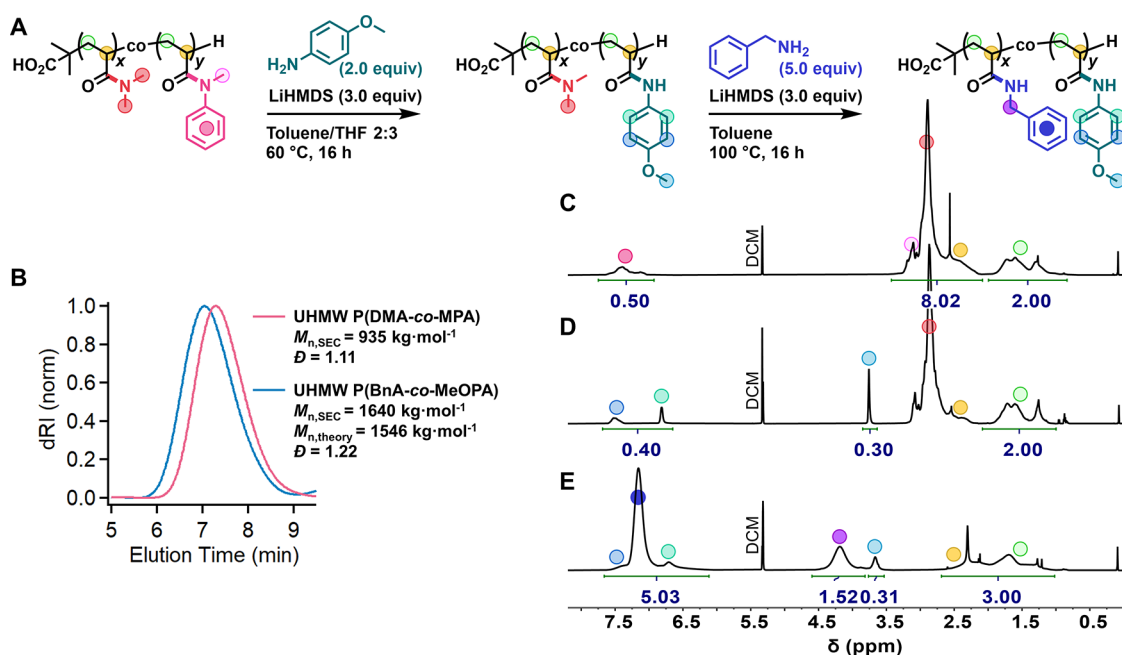


Figure 7. (A) Reaction scheme of sequential chemoselective transamidation of UHMW P(DMA-co-MPA). (B) SEC traces of UHMW P(DMA-co-MPA) prior to transamidation and UHMW P(BnA-co-MeOPA) following two-step transamidation highlighting the shift to lower elution time and concomitant increase in molecular weight. (C) ¹H NMR spectrum of UHMW P(DMA-co-MPA). (D) ¹H NMR spectrum of the UHMW P(BnA-co-MeOPA). (E) ¹H NMR spectrum of UHMW P(BnA-co-MeOPA). All spectra (600 MHz) were recorded in DCM-*d*₂.

while the *N,N*-dimethyl amides remained unaltered, as evidenced by the aromatic intensities in the transamidated copolymer (4H) aligning well with those of the starting material (5H) (Figures 7C,D and S53–S59). A subsequent reaction with benzylamine, using the previously optimized reaction conditions, yielded the doubly transamidated polymer product UHMW P(BnA-co-MeOPA) (Figures 7E and S60). Additional confirmation of the chemoselectivity between the pendant DMA and MPA moieties was provided by 2D HSQC NMR spectroscopy (Figure S62). Notably, SEC analysis showed a distinct shift to a lower elution volume, corresponding to an increase in molecular weight ($M_{n,SEC} = 1640 \text{ kg mol}^{-1}$), which aligned well with the theoretical molecular weight calculated from quantitative conversion as verified by ¹H NMR spectroscopy ($M_{n,theory} = 1546 \text{ kg mol}^{-1}$) (Figure 7B). This represents the first demonstration of a chemoselective PPM on a UHMW copolymer with an extraordinarily high DP_n of approximately 10,000.

CONCLUSIONS

In summary, we have successfully reported a novel PPM technique that utilizes the LiHMDS-mediated transamidation of unactivated tertiary amides to diversify acrylamide polymers, especially poly(*N,N*-dimethylacrylamide) (PDMA). Unlike traditional PPM approaches that require additional functional monomer synthesis and may suffer from poor atom economy and susceptibility to hydrolysis, our method makes use of the bench-stable and typically inert PDMA as a precursor polymer. The method demonstrated a broad substrate scope, tolerating amines with pendent functional groups, and achieved quantitative to moderate conversions. Building on recent advances in UHMW polymer synthesis, we unveiled new possibilities for modifying UHMW acrylamide polymers. We also demonstrated that our method could be extended to acrylamide copolymers that incorporate more activated *N*-

alkyl-*N*-aryl tertiary amides, expanding the scope to less nucleophilic aromatic amines and allowing for the chemoselective transamidation of acrylamide copolymers containing amides with differing reactivities, as ultimately exemplified on a UHMW copolymer. The current study enriches the toolset available for the precision synthesis of advanced polymers, showcasing the untapped potential of leveraging small-molecule chemistry for macromolecular modifications. Future work focuses on further expanding the substrate scope and exploring the practical applications of these newly synthesized polymers.

ASSOCIATED CONTENT

Supporting Information

The Supporting Information is available free of charge at <https://pubs.acs.org/doi/10.1021/jacs.3c12174>.

Materials, instrumentation, synthetic procedures, and additional characterization including polymerization kinetics, SEC data, and NMR spectra (PDF)

AUTHOR INFORMATION

Corresponding Author

Brent S. Sumerlin – George & Josephine Butler Polymer Research Laboratory, Center for Macromolecular Science & Engineering, Department of Chemistry, University of Florida, Gainesville, Florida 32611-7200, United States; orcid.org/0000-0001-5749-5444; Email: sumerlin@chem.ufl.edu

Authors

Lucca Trachsel – George & Josephine Butler Polymer Research Laboratory, Center for Macromolecular Science & Engineering, Department of Chemistry, University of Florida, Gainesville, Florida 32611-7200, United States; orcid.org/0000-0002-4342-1003

Debabrata Konar – George & Josephine Butler Polymer Research Laboratory, Center for Macromolecular Science & Engineering, Department of Chemistry, University of Florida, Gainesville, Florida 32611-7200, United States

Jason D. Hillman – George & Josephine Butler Polymer Research Laboratory, Center for Macromolecular Science & Engineering, Department of Chemistry, University of Florida, Gainesville, Florida 32611-7200, United States

Cullen L. G. Davidson, IV – George & Josephine Butler Polymer Research Laboratory, Center for Macromolecular Science & Engineering, Department of Chemistry, University of Florida, Gainesville, Florida 32611-7200, United States

Complete contact information is available at:

<https://pubs.acs.org/10.1021/jacs.3c12174>

Author Contributions

The manuscript was written through contributions of all authors. All authors have given approval to the final version of the manuscript.

Notes

The authors declare no competing financial interest.

ACKNOWLEDGMENTS

The work was supported by the Army Research Office through a MURI Grant (W911NF2310260). Additional support from the University of Florida is gratefully acknowledged.

REFERENCES

- (1) Günay, K. A.; Theato, P.; Klok, H.-A. Standing on the Shoulders of Hermann Staudinger: Post-Polymerization Modification from Past to Present. *J. Polym. Sci., Part A: Polym. Chem.* **2013**, *51*, 1–28.
- (2) Blasco, E.; Sims, M. B.; Goldmann, A. S.; Sumerlin, B. S.; Barner-Kowollik, C. 50th Anniversary Perspective: Polymer Functionalization. *Macromolecules* **2017**, *50*, 5215–5252.
- (3) Adili, A.; Korpusik, A. B.; Seidel, D.; Sumerlin, B. S. Photocatalytic Direct Decarboxylation of Carboxylic Acids to Derivatize or Degrade Polymers. *Angew. Chem., Int. Ed.* **2022**, *61*, No. e202209085.
- (4) Garrison, J. B.; Hughes, R. W.; Young, J. B.; Sumerlin, B. S. Photoinduced SET to Access Olefin-Acrylate Copolymers. *Polym. Chem.* **2022**, *13*, 982–988.
- (5) Larsen, M. B.; Wang, S.-J.; Hillmyer, M. A. Poly(Allyl Alcohol) Homo- and Block Polymers by Postpolymerization Reduction of an Activated Polyacrylamide. *J. Am. Chem. Soc.* **2018**, *140*, 11911–11915.
- (6) Schué, E.; Rickertsen, D. R. L.; Korpusik, A. B.; Adili, A.; Seidel, D.; Sumerlin, B. S. Alternating Styrene–Propylene and Styrene–Ethylene Copolymers Prepared by Photocatalytic Decarboxylation. *Chem. Sci.* **2023**, *14*, 11228–11236.
- (7) Gauthier, M. A.; Gibson, M. I.; Klok, H.-A. Synthesis of Functional Polymers by Post-Polymerization Modification. *Angew. Chem., Int. Ed.* **2009**, *48*, 48–58.
- (8) Boen, N. K.; Hillmyer, M. A. Post-Polymerization Functionalization of Polyolefins. *Chem. Soc. Rev.* **2005**, *34*, 267.
- (9) Das, A.; Theato, P. Activated Ester Containing Polymers: Opportunities and Challenges for the Design of Functional Macromolecules. *Chem. Rev.* **2016**, *116*, 1434–1495.
- (10) Günay, K. A.; Schüwer, N.; Klok, H.-A. Synthesis and Post-Polymerization Modification of Poly(Pentafluorophenyl Methacrylate) Brushes. *Polym. Chem.* **2012**, *3*, 2186–2192.
- (11) Van Guyse, J. F. R.; Bernhard, Y.; Podevyn, A.; Hoogenboom, R. Non-activated Esters as Reactive Handles in Direct Post-Polymerization Modification. *Angew. Chem., Int. Ed.* **2023**, *62*, No. e202303841.
- (12) Easterling, C. P.; Kubo, T.; Orr, Z. M.; Fanucci, G. E.; Sumerlin, B. S. Synthetic Upcycling of Polyacrylates through

Organocatalyzed Post-Polymerization Modification. *Chem. Sci.* **2017**, *8*, 7705–7709.

(13) Van Guyse, J. F. R.; Leiske, M. N.; Verjans, J.; Bernhard, Y.; Hoogenboom, R. Accelerated Post-Polymerization Amidation of Polymers with Side-Chain Ester Groups by Intramolecular Activation. *Angew. Chem., Int. Ed.* **2022**, *61*, No. e202201781.

(14) Kemnitz, C. R.; Loewen, M. J. Amide Resonance” Correlates with a Breadth of C–N Rotation Barriers. *J. Am. Chem. Soc.* **2007**, *129*, 2521–2528.

(15) Mucsi, Z.; Tsai, A.; Szori, M.; Chass, G. A.; Viskolcz, B.; Csizmadia, I. G. A Quantitative Scale for the Extent of Conjugation of the Amide Bond. Amidity Percentage as a Chemical Driving Force. *J. Phys. Chem. A* **2007**, *111*, 13245–13254.

(16) Li, G.; Ma, S.; Szostak, M. Amide Bond Activation: The Power of Resonance. *Trends Chem.* **2020**, *2*, 914–928.

(17) Gao, P.; Rahman, M. M.; Zamalloa, A.; Feliciano, J.; Szostak, M. Classes of Amides That Undergo Selective N–C Amide Bond Activation: The Emergence of Ground-State Destabilization. *J. Org. Chem.* **2023**, *88*, 13371–13391.

(18) Liu, Y.; Shi, S.; Achtenhagen, M.; Liu, R.; Szostak, M. Metal-Free Transamidation of Secondary Amides via Selective N–C Cleavage under Mild Conditions. *Org. Lett.* **2017**, *19*, 1614–1617.

(19) Meng, G.; Shi, S.; Lalancette, R.; Szostak, R.; Szostak, M. Reversible Twisting of Primary Amides via Ground State N–C(O) Destabilization: Highly Twisted Rotationally Inverted Acyclic Amides. *J. Am. Chem. Soc.* **2018**, *140*, 727–734.

(20) Larsen, M. B.; Herzog, S. E.; Quilter, H. C.; Hillmyer, M. A. Activated Polyacrylamides as Versatile Substrates for Postpolymerization Modification. *ACS Macro Lett.* **2018**, *7*, 122–126.

(21) Li, G.; Ji, C.-L.; Hong, X.; Szostak, M. Highly Chemoselective, Transition-Metal-Free Transamidation of Unactivated Amides and Direct Amidation of Alkyl Esters by N–C/O–C Cleavage. *J. Am. Chem. Soc.* **2019**, *141*, 11161–11172.

(22) Meng, G.; Szostak, M. Sterically Controlled Pd-Catalyzed Chemoselective Ketone Synthesis via N–C Cleavage in Twisted Amides. *Org. Lett.* **2015**, *17*, 4364–4367.

(23) Meng, G.; Lalancette, R.; Szostak, R.; Szostak, M. N-Methylamino Pyrimidyl Amides (MAPA): Highly Reactive, Electronically-Activated Amides in Catalytic N–C(O) Cleavage. *Org. Lett.* **2017**, *19*, 4656–4659.

(24) Pace, V.; Holzer, W.; Ielo, L.; Shi, S.; Meng, G.; Hanna, M.; Szostak, R.; Szostak, M. 17O NMR and 15N NMR Chemical Shifts of Sterically-Hindered Amides: Ground-State Destabilization in Amide Electrophilicity. *Chem. Commun.* **2019**, *55*, 4423–4426.

(25) Spieß, P.; Berger, M.; Kaiser, D.; Maulide, N. Direct Synthesis of Enamides via Electrophilic Activation of Amides. *J. Am. Chem. Soc.* **2021**, *143*, 10524–10529.

(26) Chen, J.; Xia, Y.; Lee, S. Coupling of Amides with Ketones via C–N/C–H Bond Cleavage: A Mild Synthesis of 1,3-Diketones. *Org. Chem. Front.* **2020**, *7*, 2931–2937.

(27) Feng, M.; Zhang, H.; Maulide, N. Challenges and Breakthroughs in Selective Amide Activation. *Angew. Chem., Int. Ed.* **2022**, *61*, No. e202212213.

(28) Hartlieb, M. Photo-Iniferter RAFT Polymerization. *Macromol. Rapid Commun.* **2022**, *43*, No. 2100514.

(29) Parkatzidis, K.; Wang, H. S.; Truong, N. P.; Anastasaki, A. Recent Developments and Future Challenges in Controlled Radical Polymerization: A 2020 Update. *Chem.* **2020**, *6*, 1575–1588.

(30) Truong, N. P.; Jones, G. R.; Bradford, K. G. E.; Konkolewicz, D.; Anastasaki, A. A Comparison of RAFT and ATRP Methods for Controlled Radical Polymerization. *Nat. Rev. Chem.* **2021**, *5*, 859–869.

(31) Jones, G. R.; Anastasaki, A.; Whitfield, R.; Engelis, N.; Liarou, E.; Haddleton, D. M. Copper-Mediated Reversible Deactivation Radical Polymerization in Aqueous Media. *Angew. Chem., Int. Ed.* **2018**, *57*, 10468–10482.

(32) Carmean, R. N.; Figg, C. A.; Scheutz, G. M.; Kubo, T.; Sumerlin, B. S. Catalyst-Free Photoinduced End-Group Removal of Thiocarbonylthio Functionality. *ACS Macro Lett.* **2017**, *6*, 185–189.

- (33) Van Guyse, J. F. R.; Verjans, J.; Vandewalle, S.; De Bruycker, K.; Du Prez, F. E.; Hoogenboom, R. Full and Partial Amidation of Poly(Methyl Acrylate) as Basis for Functional Polyacrylamide (Co)Polymers. *Macromolecules* **2019**, *52*, 5102–5109.
- (34) Verjans, J.; Sedláčik, T.; Jerca, V. V.; Bernhard, Y.; Van Guyse, J. F. R.; Hoogenboom, R. Poly(N-Allyl Acrylamide) as a Reactive Platform toward Functional Hydrogels. *ACS Macro Lett.* **2023**, *12*, 79–85.
- (35) Easterling, C. P.; Coste, G.; Sanchez, J. E.; Fanucci, G. E.; Sumerlin, B. S. Post-Polymerization Modification of Polymethacrylates Enabled by Keto–Enol Tautomerization. *Polym. Chem.* **2020**, *11*, 2955–2958.
- (36) Mucsi, Z.; Chass, G. A.; Csizmadia, I. G. Amidicity Change as a Significant Driving Force and Thermodynamic Selection Rule of Transamidation Reactions. A Synergy between Experiment and Theory. *J. Phys. Chem. B* **2008**, *112*, 7885–7893.
- (37) Feng, F.-F.; Liu, X.-Y.; Cheung, C. W.; Ma, J.-A. Tungsten-Catalyzed Transamidation of Tertiary Alkyl Amides. *ACS Catal.* **2021**, *11*, 7070–7079.
- (38) Bej, R.; Haag, R. Mucus-Inspired Dynamic Hydrogels: Synthesis and Future Perspectives. *J. Am. Chem. Soc.* **2022**, *144*, 20137–20152.
- (39) Bayer, I. S. Recent Advances in Mucoadhesive Interface Materials, Mucoadhesion Characterization, and Technologies. *Adv. Mater. Interfaces* **2022**, *9*, No. 2200211.
- (40) Wallert, M.; Nie, C.; Anilkumar, P.; Abbina, S.; Bhatia, S.; Ludwig, K.; Kizhakkedathu, J. N.; Haag, R.; Block, S. Mucin-Inspired, High Molecular Weight Virus Binding Inhibitors Show Biphasic Binding Behavior to Influenza A Viruses. *Small* **2020**, *16*, No. 2004635.
- (41) Carmean, R. N.; Becker, T. E.; Sims, M. B.; Sumerlin, B. S. Ultra-High Molecular Weights via Aqueous Reversible-Deactivation Radical Polymerization. *Chem.* **2017**, *2*, 93–101.
- (42) Carmean, R. N.; Sims, M. B.; Figg, C. A.; Hurst, P. J.; Patterson, J. P.; Sumerlin, B. S. Ultra-High Molecular Weight Hydrophobic Acrylic and Styrenic Polymers through Organic-Phase Photoiniferter-Mediated Polymerization. *ACS Macro Lett.* **2020**, *9*, 613–618.
- (43) Olson, R. A.; Lott, M. E.; Garrison, J. B.; Davidson, C. L. G.; Trachsel, L.; Pedro, D. I.; Sawyer, W. G.; Sumerlin, B. S. Inverse Miniemulsion Photoiniferter Polymerization for the Synthesis of Ultrahigh Molecular Weight Polymers. *Macromolecules* **2022**, *55*, 8451–8460.
- (44) Davidson, C. L. G. I. V.; Lott, M. E.; Trachsel, L.; Wong, A. J.; Olson, R. A.; Pedro, D. I.; Sawyer, W. G.; Sumerlin, B. S. Inverse Miniemulsion Enables the Continuous-Flow Synthesis of Controlled Ultra-High Molecular Weight Polymers. *ACS Macro Lett.* **2023**, *12*, 1224–1230.
- (45) Hie, L.; Fine Nathel, N. F.; Shah, T. K.; Baker, E. L.; Hong, X.; Yang, Y.-F.; Liu, P.; Houk, K. N.; Garg, N. K. Conversion of Amides to Esters by the Nickel-Catalysed Activation of Amide C–N Bonds. *Nature* **2015**, *524*, 79–83.
- (46) Szostak, R.; Meng, G.; Szostak, M. Resonance Destabilization in N-Acylanilines (Anilides): Electronically-Activated Planar Amides of Relevance in N–C(O) Cross-Coupling. *J. Org. Chem.* **2017**, *82*, 6373–6378.
- (47) Miyake, G. M.; Chen, E. Y.-X. Metallocene-Mediated Asymmetric Coordination Polymerization of Polar Vinyl Monomers to Optically Active, Stereoregular Polymers. *Macromolecules* **2008**, *41*, 3405–3416.
- (48) Kayık, G.; Tüzün, N. Ş. Stereoselective Propagation in Free Radical Polymerization of Acrylamides: A DFT Study. *J. Mol. Graphics Modell.* **2014**, *49*, 55–67.
- (49) Hirano, T.; Nasu, S.; Morikami, A.; Ute, K. The Effect of the N-Substituent *s*-Trans to the Carbonyl Group of N-Methylacrylamide Derivatives on the Stereospecificity of Radical Polymerizations. *J. Polym. Sci., Part A: Polym. Chem.* **2009**, *47*, 6534–6539.
- (50) Beckingham, B. S.; Sanoja, G. E.; Lynd, N. A. Simple and Accurate Determination of Reactivity Ratios Using a Nonterminal Model of Chain Copolymerization. *Macromolecules* **2015**, *48*, 6922–6930.
- (51) Bordwell, F. G.; Algrim, D. J. Acidities of Anilines in Dimethyl Sulfoxide Solution. *J. Am. Chem. Soc.* **1988**, *110*, 2964–2968.
- (52) Lipping, L.; Kütt, A.; Kaupmees, K.; Koppel, I.; Burk, P.; Leito, I.; Koppel, I. A. Acidity of Anilines: Calculations vs Experiment. *J. Phys. Chem. A* **2011**, *115*, 10335–10344.
- (53) Bordwell, F. G.; Drucker, G. E.; Fried, H. E. Acidities of Carbon and Nitrogen Acids: The Aromaticity of the Cyclopentadienyl Anion. *J. Org. Chem.* **1981**, *46*, 632–635.
- (54) Fraser, R. R.; Mansour, T. S.; Savard, S. Acidity Measurements on Pyridines in Tetrahydrofuran Using Lithiated Silylamines. *J. Org. Chem.* **1985**, *50*, 3232–3234.